COLLABORATIVE VALIDATION OF SAFE: REDUCING FALSE POSITIVES AND ENHANCING ACCURACY OF CONJUNCTION DATA MESSAGES

Davide Costigliola(1), Francesca Andreoli(1), Benedetta M. Cattani(1), Francesco Foglia(1), Simão Marto(1), Lisa De Backer(2), Davide Cavalli(2), Rooderick Ciggaar(2), and Joachim Strenge(2)

(1)*Ecosmic, Torino, Italy, Email: {davide.costigliola, francesca.andreoli, benedetta.cattani, francesco.foglia, simao.marto}@ecosmic.space*

(2)*ISISPACE, Delft, The Netherlands, Email: {l.debacker, d.cavalli, r.ciggaar, j.strenge}@isispace.nl*

ABSTRACT

Earth orbits are becoming increasingly congested, with a rapidly growing number of objects polluting the most commonly used orbital regimes. As a consequence, in the last decade, many commercial and government-driven initiatives have been put into place to ensure the long-term sustainability of outer space, with a particular focus on improving the collision avoidance process. To this end, this paper presents an innovative approach to risk analysis for situational awareness and space traffic management. The findings include results from the application of the System to Avoid Fatal Events (SAFE) to a real mission, made possible through a productive collaboration with ISISPACE. SAFE marks a substantial advancement in the field of Space Traffic Management by employing cutting-edge algorithms that provide a more accurate representation of uncertainty, by efficiently propagating that uncertainty, while accounting for non-linearities and modelling orbiting bodies using complex geometries that closely mirror real-world conditions. Furthermore, the selected case study involves an ESA and EC-funded IOD/IOV mission named CSC-1 (Σyndeo-1), demonstrating how public investment can effectively drive and support the development and validation of commercial technologies.

Keywords: Collision Avoidance; Space Situational Awareness; Space Traffic Management.

1. INTRODUCTION

In the early decades of the space age, scientific progress was the primary goal of space exploration, with little consideration for potential long-term consequences. As the number of Earth-orbiting objects increased, particularly with the rise of satellite mega-constellations, space debris mitigation became a major concern. This is particularly true in Low Earth Orbits (LEO), as described in [22]. Current estimates suggest that over 900,000 small debris objects, each with a radius of at least 1 cm, are orbiting LEO uncontrollably, posing a significant threat to operational satellites. The potential consequences of collisions between orbiting objects can be severe, as evidenced by the 2009 Iridium-33/Cosmos-2251 incident. Indeed, while satellite shielding can provide protection against smaller debris, any collision involving an active satellite and objects with a cross-section larger than 10 cm is highly likely to result in a total destruction. Furthermore, the growing number of tracked objects, both operational and non-operational, has led to a sharp rise in conjunction alerts which must be managed by operators. Millions of space conjunctions alerts are triggered annually: while most are non-critical, an increasingly congested space environment could overwhelm the existing STM capabilities, since the assessment of high-risk events is both time-consuming and resource-intensive. The situation becomes even more critical when two operational satellites are involved, due to the absence of standardized protocols, automated communication, and coordinated response procedures. Lastly, while collision avoidance manoeuvres (CAMs) are relatively inexpensive compared to other orbital manoeuvres, their increasing frequency demands additional onboard propellant and disrupts routine operations.

The primary communication channel for collision risk analysis and notifications relies on Conjunction Data Messages (CDMs), that are self-contained datasets formatted in ASCII text files using a key-value structure. Each CDM provides critical information about a conjunction event between two objects. These messages are generated whenever a conjunction is detected with an estimated collision probability exceeding a predefined threshold. Upon receiving a CDM, dedicated flight dynamics teams evaluate whether an avoidance manoeuvre is necessary to mitigate the risk of collision. The final decision balances the timing of the manoeuvre with the accuracy of the estimated collision probability. The goal is to execute the manoeuvre as soon as possible to minimize costs and maximize the spacecraft's operational time. However, the accuracy of these estimates improves only with multiple screenings (i.e., successive CDMs). Conversely, as the number of conjunction events rises, the available lead time for collision avoidance decision-making decreases. Therefore, it is essential to develop ad-

Proc. 9th European Conference on Space Debris, Bonn, Germany, 1–4 April 2025, published by the ESA Space Debris Office
Editors: S. Lemmens, T. Flohrer & F. Schmitz, (http://conference.sdo.esoc.esa.int, April 2025)

vanced technical solutions that offer precise forward visibility into the evolution of conjunction events, ensuring accurate assessments regardless of the number of screenings already conducted.
Within this context, as a result of a productive collaboration between two new space companies, ISISPACE and Ecosmic, this paper aims to present the capabilities of SAFE, an intuitive and highly accurate tool designed to help operators meet STM regulations while safeguarding their assets in orbit. SAFE allows for a better estimation of the probability of collision, shortening the decision-making time. After this introduction, Section 2 presents an overview of existing methodologies. Section 3 outlines a high-level description of SAFE, along with the benefits of this software product over traditional approaches. The close encounters experienced by CSC-1 operated by ISISPACE are detailed in Section 4. In Section 5, SAFE is validated by comparing its results with a Monte Carlo analysis. Finally, conclusions and potential future developments are outlined in Section 6.

2. OVERVIEW OF THE STATE OF THE ART

Estimating the collision risk is the first step to determine whether a collision avoidance manoeuvre is required. Such collision risk cannot be accurately assessed based solely on the satellite's nominal trajectory due to uncertainties related to orbit determination procedures and the propagation environment. Over the past few decades, many researchers have focused on calculating collision probabilities between objects, making collision probability the most commonly used metric in the field of space-object conjunction assessment. The analysis of space conjunctions is typically divided in two main steps: the propagation of the uncertainty, and the computation of the probability of collision.

2.1. Propagation of the Uncertainty

The first step involves finding the solution to the well-known Fokker-Planck equation:

$$\frac{\partial p(\boldsymbol{x},t)}{\partial t} = -\sum_{i=1}^{n} \frac{\partial}{\partial x^i}\left[p(\boldsymbol{x},t)\boldsymbol{f}^i(\boldsymbol{x},t)\right] + \frac{1}{2}\sum_{i=1}^{n}\sum_{j=1}^{n}\frac{\partial^2}{\partial x^i \partial x^j}\left[p(\boldsymbol{x},t)\boldsymbol{G}(t)^{ij}\boldsymbol{P}(t)^{ij}\boldsymbol{G}^T(t)^{ij}\right] \quad (1)$$

Equation (1) describes the time evolution of the Probability Density Function (PDF) $p(\boldsymbol{x},t)$. Various methods have been developed to address this problem. The fastest techniques, from a computational perspective, rely on linearizing the dynamics, but they often lack the necessary accuracy for examining close encounters between two objects in space. Monte Carlo sampling methods are frequently used to propagate uncertainties due to their high precision [9, 3, 16]. However, these approaches can be very time-consuming and are not suitable for operational collision avoidance. One common technique to enhance the accuracy of propagation is to approximate the probability density function (PDF). However, the effectiveness of this approach depends heavily on the dynamics propagation methods used in conjunction with it. Additionally, the dynamics themselves can also be approximated, leading to a more accurate integration of uncertainty. It is important to note that when dynamics approximation methods are used on their own, they do not offer significant advantages in terms of computational time. Dynamics approximation methods can be classified into two main groups: Taylor's integration and response surface mapping. Within the context of Taylor's expansion methods, Park and Scheers [17] used state transition tensors, which are high-order partial derivatives of the dynamics, to extract information about the final propagated uncertainty distribution arising from a deviation in the initial state. The Taylor expansion can also be computed in a computerized environment using differential algebra. In a computerized setting, a Taylor polynomial is generated, and by establishing a relationship between the final state and a perturbation of the initial state, additional information about the final uncertainty can be easily obtained. In the context of response surface mapping, the solution to the differential equations is approximated using a weighted sum of multivariate polynomials. This approach involves drawing a reduced number of samples from the initial distribution and propagating them through numerical integration. From these propagated samples, a response surface of the final state is generated as a function of a deviation from the initial state, utilizing polynomials. This technique is generic, meaning it can handle any initial distribution and is not dependent on the underlying dynamics. Related and interesting work can be found in [5, 4, 12]. It is worth mentioning that since the polynomial chaos expansion establishes the relationship between one final time and the corresponding initial state, computing the probability of collision for different epochs may become prohibitive in terms of computational time.

2.2. Computation of the Probability of Collision

The next step for the evaluation of the risk of a conjunction is to compute the probability of collision based on the propagated uncertainty. Over the past few decades, several methods have been developed for this purpose, which can be categorized into two main groups: methods for high-relative-velocity encounters (or short-term encounters) and methods for low-relative-velocity encounters (or long-term encounters). In high-relative-velocity encounters, the relative velocities of two Resident Space Objects (RSOs) are typically several kilometres per second. The time spent in the encounter region is usually only a fraction of a second or at most a few seconds. During this brief period, the effects of other forces can be ignored, allowing the relative motion between the two RSOs in the encounter region to be treated as uniform rectilinear motion. Additionally, the velocity uncertainty of both RSOs is often negligible compared to their relative velocity. Consequently, the position error ellipsoid remains stable throughout the encounter, and the position errors for the two RSOs can be represented by two uncorrelated constant covariance matrices. Low velocity encounters are common in formation flying and target-chaser scenarios, making them more and more common with the rise of mega-constellations or in-orbit servicing missions. In low-relative-velocity encounters, the assumptions of rectilinear motion made for the short-term encounter model become invalid. This is due to the significant time spent in the encounter region, which means that the relative velocity cannot be assumed to be constant. As a result, the combined error covariance matrices cannot be regarded as constant either, leading to a curved relative trajectory between the two objects.

Foster and Estes [14] developed a collision probability model using polar coordinates. They generate a combined probability density function (PDF) based on the states and covariances at the time of closest approach. To simplify the analysis of short-term encounters, the problem is reduced to two dimensions by introducing an encounter plane, which includes the relative velocity and the velocity vectors of the bodies involved. By projecting the uncertainty into this encounter plane, the probability of collision is computed by evaluating a two-dimensional integral of the combined PDF. Building on previous work, Patera [18] and Alfano [1] significantly reduced the computational load by converting the two-dimensional integration into a one-dimensional process. They achieved this by integrating along the perimeter of the hard body and utilizing error functions, respectively. Additionally, the adaptability of their algorithms was enhanced, allowing their methods to be applied not only to bodies modelled as spherical shapes, but also to a wider range of geometries. Based on the Rician probability density function (PDF), Chan [7] developed a semi-analytical method for calculating the instantaneous probability of a collision. This method involves generating an axially symmetric ellipsoid that has the same volume as the original ellipsoid. It employs a convergent infinite series for integration along two symmetrical dimensions, while the final integration along the third dimension is performed numerically. However, Chan's algorithm has several limitations. It is applicable only for small hard-ball radii (i.e., less than 100 meters) and/or position errors with standard deviations of less than tens of kilometers.

Long-term encounters can be analyzed similarly to short-term encounters. By considering the geometry of the encounter as a composition of multiple volumes, each corresponding to a different epoch, these volumes can be reduced to sections. For each section, one can calculate the two-dimensional probability of a collision as done in [18], assuming linear motion. Additionally, at each epoch, it is possible to compute a one-dimensional probability of collision along the relative velocity vector within the volume. The probability of collision for each volume is obtained by multiplying these two probabilities. Finally, the total probability of collision is simply the sum of the probabilities for all individual volumes. Patera [19] proposed a method for calculating the probability of a collision when the relative motion cannot be linearized. This approach utilizes contour integration techniques, transforming the problem into a scaled frame where the covariance matrix is symmetric. Consequently, the collision probability rate is computed and integrated over the duration of the encounter, ultimately leading to the determination of the cumulative collision probability. Although this method is remarkable and has been incorporated into the European Space Agency (ESA) software CORAM, it only addresses the effects of non-linearities in relative motion and is based on the simplifying assumption of Gaussian distributions. Coppola's method, as presented in [8], calculates the probability of a collision by integrating the flux of a combined time-dependent PDF over a predefined time window on the surface of a hard-ball sphere. This approach takes into account uncertainties in both position and velocity, although the algorithm is based on the assumption that the distributions are Gaussian. Alfano [2] proposed three methods to calculate the probability of collision by using different geometrical shapes: cylinders, adjoint parallelepipeds, and voxels. Each of these methods calculates the probability of collision through a two-dimensional integration over the sections that form the volume, combined with a one-dimensional integration along the span of the volume. The author notes that these methods are associated with a significant computational load, which makes them unsuitable for real-time applications. Instead, they are primarily intended for determining reference cases.

3. SYSTEM TO AVOID FATAL EVENTS (SAFE)

SAFE is an advanced software solution designed for efficient and reliable Space Traffic Management (STM) developed by Ecosmic. The Risk Estimation module of SAFE predicts the collision probability and miss distance between space objects. The current version of SAFE allows the operator to benefit from a refined assessment of the risk metrics (probability of collision and miss distance), based on only three information: the ID of the two objects involved in the close encounter, and the expected time of closest approach. This information can be derived from a Conjunction Data Message such as the ones produced by Space-Track and EU SST. SAFE can then harness data coming from public and commercial data providers, as well as the information coming from the users/satellite operators themselves, to calculate the risk metrics, employing its highly-performing algorithms. SAFE improves upon traditional methods by incorporating several key innovations, such as modelling non-Gaussian uncertainty, and non-linear uncertainty propagation, and keeping a full dynamical model throughout the entire encounter. For decades, uncertainty propagation has typically been performed using linear methods to reduce complexity and computational load. However, the space environment is highly non-linear, leading to significant deviations from reality when a linear approach is assumed. To achieve the desired level of accuracy, SAFE effectively incorporates these non-linear effects into the uncertainty propagation process. In orbits where relative velocities are particularly high, the encounter geometry is often linearised, and the trajectories of the bodies are assumed to follow straight lines. During such encounters, uncertainties in velocities are often neglected, and covariances are assumed to remain constant. While these assumptions may hold true for short-term encounters (such as those in Low Earth Orbit, LEO), they limit the applicability of the associated algorithms. Thanks to its new mathematical formulation, SAFE is flexible and can be applied to analyse a broader range of encounters, especially long-term ones, commonly associated with Geostationary Orbit (GEO), formation flying and close-proximity operations. Additionally, traditional methods typically assume that the bodies are spherical, which simplifies calculations but leads to an overestimation of collision probability. This overestimation results in a high number of false positives (CDMs for which an alert is raised, even if the associated risk is low), causing operators to waste significant amounts of work time. To mitigate this issue, SAFE has the capability to handle non-spherical geometries, resulting in improved accuracy and a reduction in false positives. Finally, SAFE is able to do all of that while keeping the computational time low, ensuring that it can be used in an operational environment.

4. PARAMETERS OF ANALYSED CLOSE ENCOUNTERS

In collaboration with ISISPACE, we analysed 25 CDMs for close encounters involving the satellite CSC-1 for the time period between September 6th 2024 and January 20th 2025. The physical characteristics of CSC-1 are listed in Table 2, alongside those of the other satellites involved in these conjunctions. CSC-1 is a 6U XL multi-payload spacecraft, in a low Earth orbit (LEO) which is also sun-synchronous, with the orbital parameters in Table 1.

Table 1. Orbital parameters of CSC-1

Apogee	Perigee	Inclination
548.6 km	562.0 km	97.6°

Over the time period between September 6th 2024 and January 20th 2025:

- On average, 0.2 CDMs were received per day, 1.6 days before TCA;
- The latest CDM was received 1 hour before TCA and the earliest CDM was received 3 days before TCA. 4 CDMs were created after TCA, see Fig. 1.

CDMs were aggregated into close encounter event. By definition, two CDMs pertain to the same event if they involve the same primary and secondary object and if the TCA differs by less than 20 minutes.

Over the time period analysed:

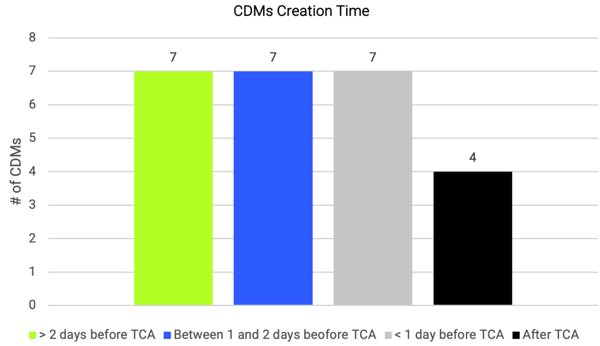

Figure 1. Time of reception of CDMs, for the selected time interval

- 18 events were identified;
- The event that generated most CDM, generated 4 of them.

The satellites involved in the analysed CDMs are listed in Table 2. CSC-1, in the first row, was the primary in all analysed conjunctions. All secondary objects, corresponding to all rows besides the first, produced a single close encounter event, apart from STARLINK-2383, which produced two events 6 hours apart. The CDMs reported potential conjunctions between CSC-1 and secondary objects from multiple owners/operators (O/O), in different proportions, as can be seen in Table 3. All secondary objects were catalogued as PAYLOADs, however not all of them were manoeuvrable. The physical properties for CSC-1 in Table 2 were provided directly from the operator. For all other objects, the reported areas are the average cross section areas provided in the DISCOS database [13]. Their mass also comes from the same database, while the hard body radius ρ is taken as the maximum value among the following fields in the DISCOS database:

- diameter
- height
- width
- depth
- span

5. MONTE CARLO ANALYSIS

To test SAFE's accuracy at estimating the probability of collision P_c, a Monte Carlo (MC) analysis [15] was performed.

Let y be the output of a system, which is given as a function f, and let $\boldsymbol{x}$ be the realisation of a random variable X, such that $y = f(\boldsymbol{x})$. Because of its dependency on a random variable, the system output y is also the realisation of a random variable Y. Throughout this document, random variables (e.g. X, Y) will be denoted with an upper-case symbol, while their realisations (e.g. $\boldsymbol{x}$, y) will be denoted with the corresponding lower-case sym-

Table 2. Satellites involved in analysed close encounters

Designator	NORAD	O/O	Manoeuvreable	Mass (kg)	Area (m^2)	ρ (m)
CSC-1	58022	ISISPACE	NO	8.34	0.035	0.466
S-NET A	43188	TU Berlin	NO	8	0.086	0.24
STARLING 1	57388	NASA	NO	12	0.098	0.5
STARLINK-1696	46545	STARLINK	YES	260	13.6	8.86
STARLINK-2163	47749	STARLINK	YES	260	13.6	8.86
STARLINK-2195	47772	STARLINK	YES	260	13.6	8.86
STARLINK-2383	47802	STARLINK	YES	260	13.6	8.86
STARLINK-2586	48390	STARLINK	YES	260	13.6	8.86
STARLINK-2755	48479	STARLINK	YES	260	13.6	8.86
STARLINK-5750	55594	STARLINK	YES	260	13.6	8.86
STARLINK-5784	56033	STARLINK	YES	305	11.1	9
STARLINK-6267	56400	STARLINK	YES	305	11.1	9
STARLINK-30310	57733	STARLINK	YES	750	33.9	29
STARLINK-30349	57713	STARLINK	YES	750	33.9	29
STARLINK-30545	58000	STARLINK	YES	750	33.9	29
STARLINK-30559	58039	STARLINK	YES	750	33.9	29
STARLINK-30759	58122	STARLINK	YES	750	33.9	29
STARLINK-30967	58416	STARLINK	YES	750	33.9	29

Table 3. Owners/Operators for the secondary objects involved in analysed close encounters

O/O	Number of CDMs	Number of events	Object type(s)	Manoeuvrable
SpaceX	20 (80%)	16 (89%)	PAYLOAD	YES
NASA	1 (4%)	1 (6%)	PAYLOAD	NO
TU Berlin	4 (16%)	1 (6%)	PAYLOAD	NO

bol. The realised variables will be written in bold if they correspond to vector quantities, e.g. $\boldsymbol{x}$.

5.1. Basics of Monte Carlo

With a MC analysis, the mean of Y, $\mu_Y = \mathrm{E}\{Y\}$, is estimated by sampling X with a high number of samples N, and computing the sample mean. [15] For example, the mean can be estimated as

$$\mu_Y \approx \overline{Y} = \frac{1}{N}\sum_{i=1}^{N} f(X_i) \tag{2}$$

where $X_1, \ldots, X_n$ form a i.i.d. sample of X.

Since the MC estimate $\overline{Y}$ depends on random variables X_i, it is itself a random variable, with a probability distribution with its own mean and variance. Since the above is an unbiased estimator, it holds that $\mathrm{E}\{\overline{Y}\} = \mu_Y$, while its standard deviation $\sigma\{\overline{Y}\}$ is given by [15]

$$\sigma_{\overline{Y}} = \frac{\sigma_Y}{\sqrt{N}} \tag{3}$$

where σ_Y is the standard deviation of Y.

As a result of the central limit theorem [10], as N grows, the distribution of $\overline{Y}$ approaches a Gaussian distribution. For such a distribution, one can use the three sigma rule, which states that 99.7% of realisations of a variable are within 3 standard deviations of the mean, i.e. $P(\mu_Y - 3\sigma_{\overline{Y}} \leq \overline{Y} \leq \mu_Y + 3\sigma_{\overline{Y}}) \approx 99.7\%$, which can also be written as $P(\overline{Y} - 3\sigma_{\overline{Y}} \leq \mu_Y \leq \overline{Y} + 3\sigma_{\overline{Y}}) \approx 99.7\%$. As such, the interval $\left[\overline{Y} - 3\sigma_{\overline{Y}}, \overline{Y} + 3\sigma_{\overline{Y}}\right]$ is used as a confidence interval on the value estimated by the MC approach.

5.2. Estimating the Probability of Collision with Monte Carlo

In our application, $X = (X_{01}, X_{02})$ represents the initial states, given at times t_{01} and t_{02}, for the primary and secondary, so that the random variable is $X = (X_{01}, X_{02})$. Let $\boldsymbol{x}(t) = \boldsymbol{\phi}(\boldsymbol{x}_0, t_0, t)$ represent the propagation of the initial state $\boldsymbol{x}_0$ at time t_0 to time t, resulting in the state of that object at time t, $\boldsymbol{x}(t)$, where $\boldsymbol{\phi}$ is the state transition function, which is the function that solves the ODE:

$$\frac{\mathrm{d}\boldsymbol{\phi}(\boldsymbol{x}_0, t_0, t)}{\mathrm{d}t} = \boldsymbol{f}\left(\boldsymbol{\phi}(\boldsymbol{x}_0, t_0, t), t\right) \tag{4}$$

$$\boldsymbol{\phi}(\boldsymbol{x}_0, t_0, t_0) = \boldsymbol{x}_0 \tag{5}$$

For the purposes of estimating the probability of collision, Y is a boolean, i.e., true-or-false variable, following a Bernoulli distribution whose parameter is the probability of collision, i.e. $Y \sim \mathrm{Bernoulli}(P_c)$. Its value indicates whether the two objects came within a distance below the hard-ball radius, defined as the sum $R = \rho_1 + \rho_2$

of the hard body radii of both objects. The formal definition of Y can be written as

$$Y = \left(\min_t \|\boldsymbol{\phi}(X_{01}, t_{01}, t) - \boldsymbol{\phi}(X_{02}, t_{02}, t)\|\right) \leq R \tag{6}$$

where the inequality results in $y = 1$ when it holds true, and $y = 0$ otherwise.

With a MC approach, the probability of collision, which is both the Bernoulli distribution parameter and the mean of Y, i.e. $P_c = \mathrm{E}\{Y\}$, is estimated as

$$P_c \approx \hat{P}_C = \frac{1}{N}\sum_{i=1}^{N}\left(\min_t \|\boldsymbol{\phi}(X_{01,i}, t_{01}, t) - \boldsymbol{\phi}(X_{02,i}, t_{02}, t)\| \leq R\right) \tag{7}$$

where samples $X_{01,i}$ and $X_{02,i}$ are obtained by sampling the respective distributions independently, as the initial states of both objects are assumed to be independent.

The distributions of the initial states, X_{01} and X_{02}, are presently assumed Gaussians, i.e. $X_{01} \sim \mathcal{N}(\boldsymbol{\mu}_{01}, \Sigma_{01})$ and $X_{02} \sim \mathcal{N}(\boldsymbol{\mu}_{02}, \Sigma_{02})$, and

$$X = (X_{01}, X_{02}) \sim \mathcal{N}\left(\begin{bmatrix}\boldsymbol{\mu}_{01}\\ \boldsymbol{\mu}_{02}\end{bmatrix}, \begin{bmatrix}\Sigma_{01} & \mathbf{0}\\ \mathbf{0} & \Sigma_{02}\end{bmatrix}\right) \tag{8}$$

Since $Y \sim \mathrm{Bernoulli}(P_c)$, its standard deviation is known to be given by

$$\sigma_Y = \sqrt{P_c(1 - P_c)} \tag{9}$$

and as such the standard deviation of the MC estimate $\hat{P}_C$ is

$$\sigma_{\hat{P}_C} = \sqrt{\frac{P_c(1 - P_c)}{N}} \tag{10}$$

Monte Carlo is a conceptually simple way to test the response of a system to uncertain inputs. Its conceptual simplicity, in additional to the theoretical confidence interval given by $\sigma_{\hat{P}_C}$ however, makes it a good benchmark against which to test our method. However, this comes at the expense of being very slow, due to the slow convergence of this method, resulting from the square-root dependency of $\sigma_{\hat{P}_C}$ with N. This means that if we want a result that is 10 times as precise, we need 100 times more samples. As such, we use MC only as a benchmark to our main SAFE algorithm.

Furthermore, to compute the $3\sigma_{\hat{P}_C}$ bounds, the value of $\sigma_{\hat{P}_C}$ is approximated using $\hat{P}_C$ in place of P_c, since the latter can only be estimated and not known exactly.

5.3. Orbital Dynamics

The model of orbital dynamics used defines the function $\mathbf{f}$. The state $\mathbf{x}$ is represented by the position $\mathbf{r}$ and velocity $\mathbf{v}$ of each object, i.e. $\mathbf{x} = (\mathbf{r}, \mathbf{v})$, in the GCRF [20], an Earth-centred inertial reference frame. The dynamics are written as $\mathbf{f}(\mathbf{x}) = \mathbf{f}(\mathbf{r}, \mathbf{v}) = (\mathbf{v}, \mathbf{a})$ where $\mathbf{a}$ is the acceleration. The acceleration is a sum of the point-mass acceleration from the Earth plus the following perturbations:

- Spherical harmonics, with degree and order up to 6X6
- Drag, with a constant ballistic coefficient B_C and the NRLMSISE-00 atmospheric model
- Third-body perturbations from the Sun and Moon

The ballistic coefficient used to model drag is defined as

$$B_C = \frac{C_D A}{m} \tag{11}$$

where A and m are the area and mass reported in Table 2, and the drag coefficient C_D is taken as 2.2.

The integration ϕ of the dynamics in $\mathbf{f}$ is obtained using a variable step Runge-Kutta method. The acceleration model and its integration are implemented using the Python library tudatpy [11].

5.4. Results

The CDMs relating to the close encounters described in Section 4 were used to obtain the MC benchmark. For all MC tests, $N = 10^6$. The Monte-Carlo analysis was run for each received CDM, of which, as mentioned, there were multiple for some events. The parameters $\boldsymbol{\mu}_{01}$, $\boldsymbol{\mu}_{02}$, Σ_{01}, and Σ_{02} are taken from the contents of the CDM.

In the following analysis, $P_{c,\ \mathrm{threshold}} = 10^{-4}$ was used as the threshold for P_c above which the CDMs or events should be regarded as critical. In this paper, those CDMs or events are said to be actionable. Sections 5.4.1 to 5.4.3 discuss the results using for the hard body radius ρ the values from the operator for CSC-1 and from DISCOS for the other objects, as described in Section 4 and shown in Table 2. Section 5.4.4 then shows results obtained with different values for ρ, including a choice that appears to be what is used by SpaceTrack, to allow a more direct comparison between the two methods. Table 4 contains all the numerical results discussed in this Section.

Table 4 shows under "SAFE HBR", SAFE's estimate of the P_c, and the MC benchmark value with its $3\sigma_{\overline{Y}}$ bounds, and under "ST" is SpaceTrack's value. The data under "CDM Operator + EVR" and "CDM EVR" were obtained with different choices of hard body radius, and are described and discussed in Section 5.4.4. All values shown in Table 4 were multiplied by 10^4, for ease of reading, and so that values greater than 1 represent $P_c > P_{c,\ \mathrm{threshold}}$, and vice-versa. When there were fewer than 10 collisions out of the 10^6 simulations that were run, it was considered that neither the value given by MC nor the resulting bounds were reliable, and as such those entries were omitted (represented with a '—'). With such few collision cases, the Gaussianity as-

Table 4. Probability of collision estimates, multiplied by 10^4, using different hard body radii, for MC and SAFE, alongside SpaceTrack's value (ST)

		SAFE HBR		CDM Operator + EVR		CDM EVR		
CDM	Secondary	MC	SAFE	MC	SAFE	MC	SAFE	ST
1	STARLINK-30759	3.10 ± 0.53	2.91	1.82 ± 0.40	1.72	0.36 ± 0.18	0.34	0.43
2	STARLING 1	—	< 0.005	—	< 0.005	—	< 0.005	< 0.005
3	STARLINK-5750	1.41 ± 0.36	1.42	3.68 ± 0.58	3.73	1.77 ± 0.40	1.64	2.08
4	STARLINK-5750	1.43 ± 0.36	1.51	3.84 ± 0.59	3.95	1.71 ± 0.39	1.73	2.20
5	STARLINK-5784	6.34 ± 0.76	6.60	16.69 ± 1.22	16.82	7.03 ± 0.80	7.37	9.38
6	STARLINK-5784	25.95 ± 1.53	25.75	63.91 ± 2.39	65.40	28.85 ± 1.61	28.73	36.55
7	STARLINK-30967	10.46 ± 0.97	10.10	6.12 ± 0.74	5.93	1.27 ± 0.34	1.14	1.46
8	S-NET A	—	0.03	2.06 ± 0.43	2.06	5.93 ± 0.73	5.71	7.12
9	S-NET A	—	0.03	2.06 ± 0.43	2.06	5.93 ± 0.73	5.71	7.12
10	S-NET A	—	0.01	0.78 ± 0.26	0.83	2.38 ± 0.46	2.31	2.95
11	S-NET A	—	< 0.005	0.36 ± 0.18	0.36	0.96 ± 0.29	0.99	1.26
12	STARLINK-30559	15.91 ± 1.20	16.02	9.11 ± 0.91	9.46	1.75 ± 0.40	1.84	2.36
13	STARLINK-30545	21.89 ± 1.40	20.81	11.89 ± 1.03	11.50	1.85 ± 0.41	2.05	2.63
14	STARLINK-30310	27.84 ± 1.58	27.86	16.65 ± 1.22	16.21	3.13 ± 0.53	3.10	3.95
15	STARLINK-1696	17.92 ± 1.27	17.40	46.01 ± 2.03	45.37	20.25 ± 1.35	19.99	25.48
16	STARLINK-1696	17.92 ± 1.27	17.40	46.01 ± 2.03	45.37	20.22 ± 1.35	19.99	25.48
17	STARLINK-2195	1.54 ± 0.37	1.50	3.89 ± 0.59	3.92	1.73 ± 0.39	1.72	2.20
18	STARLINK-2195	1.55 ± 0.37	1.50	3.88 ± 0.59	3.92	1.74 ± 0.40	1.72	2.20
19	STARLINK-2163	103.61 ± 3.04	103.18	267.83 ± 4.84	268.05	118.61 ± 3.25	118.52	150.57
20	STARLINK-2755	0.80 ± 0.27	0.70	2.02 ± 0.43	1.84	0.93 ± 0.29	0.80	1.02
21	STARLINK-2586	0.81 ± 0.27	0.78	2.01 ± 0.43	2.05	0.90 ± 0.28	0.90	1.15
22	STARLINK-30349	94.05 ± 2.90	93.25	56.31 ± 2.24	55.56	10.78 ± 0.98	10.92	13.89
23	STARLINK-6267	5.10 ± 0.68	5.47	13.89 ± 1.12	13.72	5.77 ± 0.72	6.10	7.80
24	STARLINK-2383	1.49 ± 0.37	1.59	3.99 ± 0.60	4.17	1.81 ± 0.40	1.83	2.33
25	STARLINK-2383	1.52 ± 0.37	1.38	3.82 ± 0.59	3.58	1.76 ± 0.40	1.59	2.01

sumption for $\hat{P}_c$ is not valid, which results in bounds that include negative values.

For CDMs involving S-NET A or STARLING 1 as the secondary, fewer than 10 of the sample runs of the MC analysis resulted in collisions, making the $3\sigma_{\hat{P}_c}$ bounds unreliable, which is why the bounds were not included for those entries. For all other CDMs, SAFE's estimate of P_c is within the $3\sigma_{\hat{P}_c}$ bounds. The P_c value computed by SAFE is always closer than Space-Track's (ST) estimate to the value calculated by the Monte Carlo method $\hat{P}_c$ for all CDMs analysed.

We highlight two observed scenarios:

- The P_c computed by SAFE is higher than the one provided by Space-Track. Space-Track has underestimated the Probability of Collision, and a conjunction might be discarded even if it breaches the accepted risk threshold and the Operator's satellite is under threat.
- The P_c computed by SAFE is lower than the one provided by Space-Track. Space-Track has overestimated the Probability of Collision, potentially leading the Operator to plan unnecessary Collision Avoidance Manoeuvres, which result in additional workload for the Operators and waste of fuel. These are commonly regarded as "false alerts".

5.4.1. Underestimation of the Risk

In 24% of the analysed CDMs the P_c was underestimated by Space-Track.

In particular, among the 25 CDMs analysed, there was 1 instance, CDM 1, in which Space-Track predicted the P_c to be lower than 10^{-4}, while SAFE and the Monte Carlo method computed a P_c value above the actionability threshold. In this critical occasion the Operator was not aware of the high risk that its satellite was exposed to, because Space-Track did not inform them about the threat affecting its assets.

5.4.2. Overestimation of the Risk

In 76% of the analysed CDMs, the P_c was overestimated by Space-Track.

Considering SAFE's P_c estimates, 18 (i.e. 72%) of the CDMs processed were classified as actionable, as op-

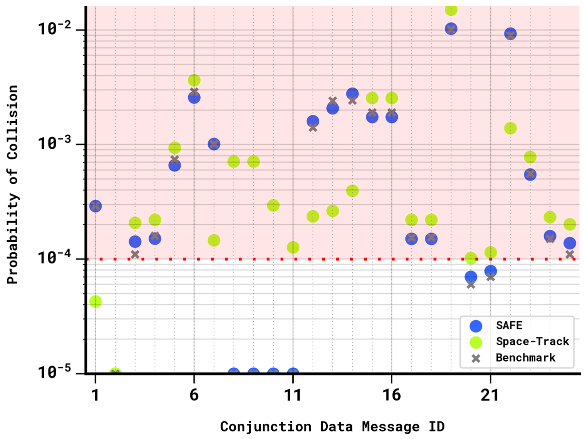

Figure 2. Scatter plot, with logarithmic scale, comparing the estimates of P_C from SAFE, SpaceTrack, and the MC benchmark

posed to the 23 (i.e. 92%) actionable CDMs predicted by Space-Track.

As can be seen in Fig. 2, there were 6 instances in which Space-Track predicted the P_c to be higher than the actionability threshold of 10-4 while SAFE and Monte Carlo estimated it to be below this value.

As the number of space debris and therefore of potential conjunctions is set to increase in the foreseeable future, having an algorithm that can accurately and timely estimate the Probability of Collision and discard false alerts is fundamental to run safe and efficient operations.

Figure 3 shows the P_c evolution of the actionable conjunction between CSC-1 and S-NET A from TU Berlin, with TCA at 2024-11-06 01:31:32 UTC, comprising CDMs 8-11. SAFE catalogued the event as non-actionable from the first CDM. In fact, although the P_c in the last CDM from Space-Track is still slightly above 10^{-4}, this was received more than 24 hours before TCA, and no CDM for this conjunction was generated afterwards, leading us to believe that the debris left the screening volume of CSC-1. In this case, CDM 8 was generated 1 day before CDM 11, which means that the Operator would have been able to discard the CDM immediately, 24 hours in advance with respect to Space-Track.

5.4.3. Error Analysis

Finally, to highlight SAFE's PC estimation accuracy and reliability, the absolute and relative error between the PC values computed by SAFE and Space-Track with respect to the Monte Carlo benchmark are plotted in Figs. 4 and 5.

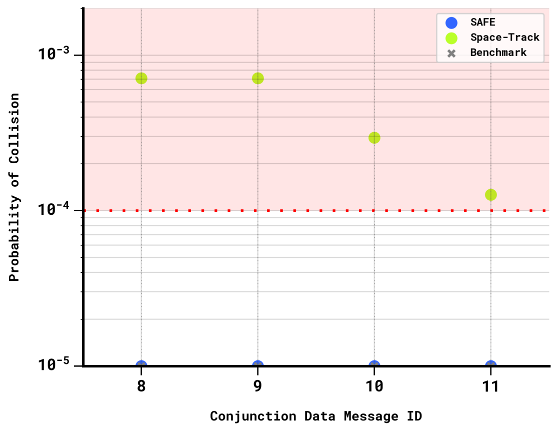

Figure 3. Estimates of P_c for Event 3

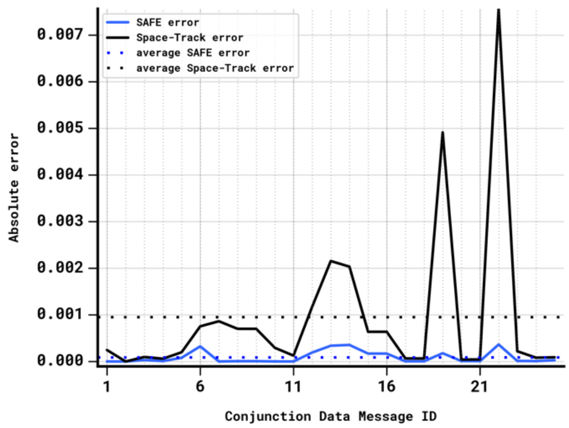

Figure 4. Absolute error of SAFE and SpaceTrack estimates compared with the MC benchmark

5.4.4. Effect of Choice of Hard Body Radius

According to the Spaceflight Safety Handbook for Satellite Operators [21], CDMs issued by SpaceTrack have fields containing the "Exclusion Volume Radius" (EVR), the "Area PC", and the "Operator Hard Body Radius" (Operator HBR), all of which are said to be useful to compute P_c. The same text suggests that the EVR is what is used to compute the PC provided by SpaceTrack. The following descriptions come from the handbook (the relevant Blue Book [6] only mentions Area PC):

- "[The EVR is] the radius of a sphere in meters to create a spherical volume representative of the object and used in the PoC calculation", and also "Pre-assigned default values for payloads and platforms (5 meters), rocket bodies and unknown objects (3 meters) and debris (1 meter) were determined through a study of sizes of objects in the space object catalog and are normally used."
- "[The Area PC] could be known by the owner/operator of the satellite or defined by

Table 5. Hard body radius values from different sources, in metres

	DISCOS					CDM	
NORAD	Heigth	Width	Depth	Span	SAFE	Operator HBR	EVR
CSC-1	0.30	0.20	0.20	0.50	0.47	—	5.00
S-NET A	0.24	0.24	0.24	0.24	0.24	1.00	5.00
STARLING 1	0.30	0.20	0.20	0.50	0.50	—	5.00
STARLINK-1696	0.10	3.70	1.50	8.86	8.86	10.11	5.00
STARLINK-2163	0.10	3.70	1.50	8.86	8.86	10.11	5.00
STARLINK-2195	0.10	3.70	1.50	8.86	8.86	10.11	5.00
STARLINK-2383	0.10	3.70	1.50	8.86	8.86	10.11	5.00
STARLINK-2586	0.10	3.70	1.50	8.86	8.86	10.11	5.00
STARLINK-2755	0.10	3.70	1.50	8.86	8.86	10.11	5.00
STARLINK-30310	0.30	4.10	2.70	29.00	29.00	17.66	5.00
STARLINK-30349	0.30	4.10	2.70	29.00	29.00	17.66	5.00
STARLINK-30545	0.30	4.10	2.70	29.00	29.00	17.66	5.00
STARLINK-30559	0.30	4.10	2.70	29.00	29.00	17.66	5.00
STARLINK-30759	0.30	4.10	2.70	29.00	29.00	17.66	5.00
STARLINK-30967	0.30	4.10	2.70	29.00	29.00	17.66	5.00
STARLINK-5750	0.10	3.70	1.50	8.86	8.86	10.11	5.00
STARLINK-5784	0.20	2.80	2.80	9.00	9.00	10.11	5.00
STARLINK-6267	0.20	2.80	2.80	9.00	9.00	10.11	5.00

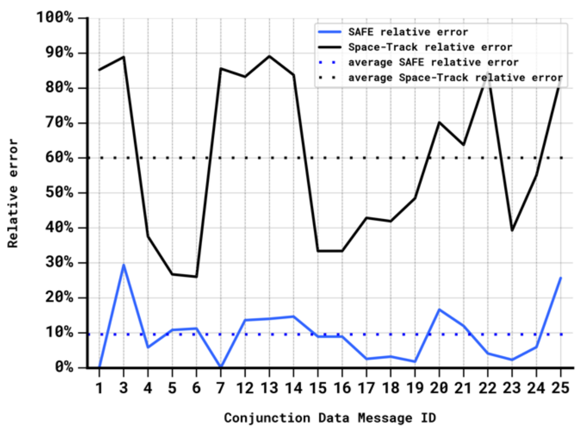

Figure 5. Relative error of SAFE and SpaceTrack estimates compared with the MC benchmark

using a Radar Cross Section (RCS) as in the case of debris. (...) This parameter can be useful for calculation collision probability.”

- “[The Operator HBR,] if input by an owner/operator, is the Hard Body Radius of the object”

Since all objects involved in the analysed conjunctions were payloads, the EVR reported in the CDMs is always $5\,\mathrm{m}$. When running SAFE, for some objects we have obtained from the operators information which includes their hard body radius. When that information is not available, the largest dimension in the DISCOS database is used. In these CDMs, we only have direct access to the HBR of CSC-1.

Table 5 shows the value of relevant quantities available in DISCOS, in the CDMs, and the value SAFE uses by default. Table 4 shows the values of the PC obtained using different sources of informations. The estimates used by SAFE by default are under ‘SAFE HBR’. The handbook [21] states that the EVR is used to compute the PC, so SAFE and the MC analysis are also run using this value of the hard body radius ρ, corresponding to the results in Table 4 under ‘CDM EVR’. It is not completely clear, however, whether the Operator HBR is also used, since the handbook [21] also states “If an O/O chooses to provide the Hard Body Radius (HBR) of their satellite on Space-Track, this can be used in the calculation of Pc”, so values using the Operator HBR given in the CDM are also shown in Table 4, under ‘CDM Operator + EVR’. The ‘+ EVR’ in the column name is because for the two objects for which the Operator HBR was not present in the CDMs the EVR was used.

The results in Table 4 show that SpaceTrack’s values are much more consistent with those under “EVR” than the other columns, suggesting that is the value they use. Considering that this value is not accurate, since it was always $5\,\mathrm{m}$ for all objects being considered, simply having access to a more accurate source of data for this value allows improving these estimates, and represents on its own a benefit of using software like SAFE compared to using SpaceTrack’s value. The cases of underestimation/overestimation of the risk discussed previously are mostly attributable to the different choices of ρ, see e.g. CDMs 3-5, which are only marked as actionable when the unrealistically high value for ρ in the EVR is used, and which become a negligible risk when more realistic values are used.

Even when comparing SpaceTrack with SAFE and MC using only the EVR as ρ, however, we see that SpaceTrack consistently overestimates P_c by 20-29%, while

SAFE is always close to the MC value, showing that SAFE's improvement upon the SpaceTrack value is not attributable solely to the more accurate choise of hard body radius, but also results from a more accurate algorithm for the computation of P_c.

6. CONCLUSIONS

This paper showed some novel results of the System to Avoid Fatal Events (SAFE) tool for conjunction analysis. SAFE marks a substantial advancement in the field of STM by employing cutting-edge algorithms that provide a more accurate representation of uncertainty, by efficiently propagating that uncertainty while accounting for non-linearities in the orbital propagation. Additionally, SAFE demonstrates exceptional flexibility and computational efficiency, enabling it to effectively handle any type of encounter. The results presented in this work demonstrate SAFE's ability to improve upon SpaceTrack's estimates of the probability of collision. SAFE analysed different close encounters involving CSC-1; for every CDM, the probability of collision computed by SAFE has been shown to closely agree with the corresponding values obtained using the Monte Carlo simulation, and to improve upon the accuracy of the computation performed by SpaceTrack. In particular, there was an occasion in which SAFE accurately predicted a high risk event that SpaceTrack missed. Moreover, in 76% of the analysed CDMs, Space-Track overestimated the probability of collision, while SAFE computed it more accurately. This is a very important result, as it directly translates to a reduction in operational workload and waste of resources.

It is worth highlighting that SAFE's average runtime is 1-2 minutes. This ensures that the Operator can have a refined P_c estimation timely available in whatever circumstance. Another advantage of SAFE's more accurate P_c estimation is that false alerts and concerning conjunctions can be reliably spotted earlier on than with Space-Track.

ACKNOWLEDGMENTS

The CSC-1 (Σyndeo-1) mission has been developed by ISISPACE with funding by the European Union. The views expressed herein can in no way be taken to reflect the official opinion of the European Union or the European Space Agency.

REFERENCES

1. Alfano S. "A numerical implementation of spherical object collision probability". In: *The Journal of the Astronautical Sciences* 53 (2005), pp. 103–109.
2. Alfano S. "Addressing nonlinear relative motion for spacecraft collision probability". In: *AIAA/AAS astrodynamics specialist conference and exhibit*. 2006, p. 6760.
3. Armellin R et al. "Rigorous computation of orbital conjunctions". In: *Advances in Space Research* 50.5 (2012), pp. 527–538.
4. Bhusal R and Subbarao K. "Generalized polynomial chaos expansion approach for uncertainty quantification in small satellite orbital debris problems". In: *The Journal of the Astronautical Sciences* 67 (2020), pp. 225–253.
5. Bhusal R and Subbarao K. "Uncertainty quantification using generalized polynomial chaos expansion for nonlinear dynamical systems with mixed state and parameter uncertainties". In: *Journal of Computational and Nonlinear Dynamics* 14.2 (2019), p. 021011.
6. CCSDS. "Conjunction Data Message". In: (2013). URL: `https://public.ccsds.org/Pubs/508x0b1e2c2.pdf`.
7. Chan K. "Collision probability analysis for earth orbiting satellites". In: *Space cooperation into the 21 st century* (1997), pp. 1033–1048.
8. Coppola VT et al. "Including velocity uncertainty in the probability of collision between space objects". In: *AAS/AIAA Spaceflight Mechanics Meeting*. Vol. 143. American Astronautical Soc. 2012, pp. 2159–2178.
9. De Vries W and Phillion D. *Monte Carlo method for collision probability calculations using 3D satellite models*. Tech. rep. Lawrence Livermore National Lab.(LLNL), Livermore, CA (United States), 2010.
10. Dekking FM. *A Modern Introduction to Probability and Statistics: Understanding why and how*. Springer Science & Business Media, 2005.
11. Dirkx D et al. "the open-source astrodynamics tudatpy software–overview for planetary mission design and science analysis". In: *EPSC2022* EPSC2022-253 (2022).
12. Doostan A and Owhadi H. "A non-adapted sparse approximation of PDEs with stochastic inputs". In: *Journal of Computational Physics* 230.8 (2011), pp. 3015–3034.
13. ESA. *DISCOS (Database and Information System Characterising Objects in Space)*. 1999. URL: `https://discosweb.esoc.esa.int/` (visited on 03/01/2025).
14. Foster JL and Estes HS. "A parametric analysis of orbital debris collision probability and maneuver rate for space vehicles. NASA". In: *National Aeronautics and Space Administration, Lyndon B. Johnson Space* (1992).
15. MacKay DJ. *Information theory, inference and learning algorithms*. Cambridge university press, 2003.

16. Morselli A et al. “A high order method for orbital conjunctions analysis: Monte Carlo collision probability computation”. In: *Advances in Space Research* 55.1 (2015), pp. 311–333.
17. Park RS and Scheeres DJ. “Nonlinear semi-analytic methods for trajectory estimation”. In: *Journal of guidance, control, and dynamics* 30.6 (2007), pp. 1668–1676.
18. Patera RP. “General method for calculating satellite collision probability”. In: *Journal of Guidance, Control, and Dynamics* 24.4 (2001), pp. 716–722.
19. Patera RP. “Satellite collision probability for nonlinear relative motion”. In: *Journal of Guidance, Control, and Dynamics* 26.5 (2003), pp. 728–733.
20. Petit G, Luzum B, et al. “IERS conventions (2010)”. In: (2010).
21. SPACE J. *Spaceflight Safety Handbook for Satellite Operators*. Version 1.7. Apr. 2023. URL: https://www.space-track.org/documents/SFS_Handbook_For_Operators_V1.7.pdf (visited on 01/29/2025).
22. Uriot T et al. “Spacecraft collision avoidance challenge: Design and results of a machine learning competition”. In: *Astrodynamics* (2022), pp. 1–20.